Journal of Power Sources 196 (2011) 9270–9275

Contents lists available at ScienceDirect

Journal of Power Sources

journal homepage: www.elsevier.com/locate/jpowsour

PdCo supported on multiwalled carbon nanotubes as an anode catalyst in a microfluidic formic acid fuel cell

D. Morales-Acosta [a], M.D. Morales-Acosta [b], L.A. Godinez [a], L. Álvarez-Contreras [c], S.M. Duron-Torres [d], J. Ledesma-García [a], L.G. Arriaga [a,*]

[a] Centro de Investigación y Desarrollo Tecnológico en Electroquímica, 76703 Querétaro, Mexico
[b] Centro de Investigación y de Estudios Avanzados del IPN., Unidad Querétaro, 76001 Querétaro, Mexico
[c] Centro de Investigación en Materiales Avanzados, Laboratorio Nacional de Nanotecnología, 31109 Chihuahua, Mexico
[d] Unidad Académica de Ciencias Químicas-Siglo XXI, Universidad Autónoma de Zacatecas, 98160 Zacatecas, Mexico

ARTICLE INFO

Article history:
Received 23 June 2011
Accepted 18 July 2011
Available online 23 July 2011

Keywords:
Microfluidic fuel cell
Formic acid
PdCo anode catalyst
MWCNTs

ABSTRACT

This work reports the synthesis of Pd-based alloys of Co and their evaluation as anode materials in a microfluidic formic acid fuel cell (μFAFC). The catalysts were prepared using the impregnation method followed by thermal treatment. The synthesized catalysts contain 22 wt.% Pd on multiwalled carbon nanotubes (Pd/MWCNT) and its alloys with two Co atomic percent in the sample with 4 at.% Co (PdCo1/MWCNT) and 10 at.% Co (PdCo2/MWCNT). The role of the alloying element was determined by XRD and XPS techniques. Both catalysts were evaluated as anode materials in a μFAFC operating with different concentrations of HCOOH (0.1 and 0.5 M), and the results were compared to those obtained with Pd/MWCNT. A better performance was obtained for the cell using PdCo1/MWCNT (1.75 mW cm^{-2}) compared to Pd/MWCNT (0.85 mW cm^{-2}) in the presence of 0.5 M HCOOH. By means of external electrode measurements, it was also possible to observe shifts in the formic acid oxidation potential due to a fuel concentration increment (ca. 0.05 V for both PdCo1/MWCNT and PdCo2/MWCNT catalysts and 0.23 V for Pd/MWCNT) that was attributed to deactivation of the catalyst material. The maximum current densities obtained were 8 mA cm^{-2} and 5.2 mA cm^{-2} for PdCo2/MWCNT and Pd/MWCNT, respectively. In this way, the addition of Co to the Pd catalyst was shown to improve the tolerance of intermediates produced during formic acid oxidation that tend to poison Pd, thus improving the catalytic activity and stability of the cell.

1. Introduction

Microfluidic fuel cells (μFCs) have received much attention in recent years due to their potential applications in the replacement of batteries in portable electronic devices (e.g., cell phones, laptops and sensors). In small electronics applications, lifetime, cost, size and weight of the power source are critical aspects of the overall system value. Therefore, μFCs offer the advantages of much higher energy density storage capacity and the ability to be recharged by replacing the fuel cartridge.

In addition, μFCs have several advantages over proton exchange membrane fuel cells (PEMFCs). A μFC, for instance, eliminates membrane-related ohmic losses, its fabrication and the relevant water management are simpler, and because it can be miniaturized, the use of liquid fuels with high energy density results in easier management and storage. The performance of μFCs is based on the laminar flow of fluids in a microchannel (at low Reynolds number (<10)) that limits convective mixing and reduces unwanted fuel crossover. The fuel and oxidant are fed in parallel microchannels, and the liquid-liquid interface produced allows for proton diffusion, avoiding the need of a polymeric membrane. In addition, the compositions of the fuel and oxidant streams (i.e., pH) can be independently selected, thus allowing the improvement of reaction kinetics and open cell potentials [1].

It is also important to note that when the current densities obtained in these systems (employing methanol, dissolved hydrogen or formic acid as fuel) are satisfactory, the corresponding values tend to be limited by mass transport effects due to the reduced diffusivity of oxygen in aqueous media. To deal with this problem, we recently proposed the use of an O_2 saturation setup that employs an acidic fluid and an O_2 gas stream [22].

Although this type of fuel cell offers exciting potential for use in future micro-electronic devices, more research is needed for the development of better electrooxidation catalysts for

* Corresponding author. Tel.: +52 442 211 6069; fax: +52 442 211 6000.
E-mail address: larriaga@cideteq.mx (L.G. Arriaga).

0378-7753/$ – see front matter © 2011 Elsevier B.V. All rights reserved.
doi:10.1016/j.jpowsour.2011.07.064

convenient fuels such as formic acid. In this regard, Pd electrodes are very active for formic acid oxidation, with higher current densities than Pt electrodes [3]. Oxidation occurs almost exclusively through a direct oxidation pathway to CO_2, without formation of species that might poison the catalyst surface. Zhou et al. [4], studied the activity of unsupported Pd nanoparticles, and they revealed a relationship between particle size and catalytic activity, finding that more reactive catalysts consist of the smallest Pd nanoparticles (9 and 11 nm). Research in Pd catalysis has mainly focused on addressing Pd deactivation promoted by adsorption of formic acid oxidation by-products. From this research, enhanced activity has been achieved by alloying a second metal to palladium. The study of the resulting bimetallic catalysts, such as Pd–Au [5], Pd–Ni [6], Pd–Pt [7], Pd–Ir [8], Pd–Pb [9] and Pd–Sn [10], has shown that it is possible to reduce or eliminate the limitations previously described, probably due to a bifunctional mechanism as well as structural or electronic effects.

Recently, our research group synthesized and evaluated Pd and PdCo catalysts on multiwalled carbon nanotubes (MWCNTs), and their electrocatalytic activity was investigated in the context of formic acid electrooxidation. The results obtained from voltamperometric studies showed that a PdCo/MWCNT catalyst has a current density three times greater than that achieved with a Pd/MWCNT catalyst. In addition, the oxidation potential of formic acid on PdCo/MWCNT was shifted ca. 50 mV lower as compared to Pd/MWCNT [11].

This work describes the results of a performance evaluation of PdCo on multiwalled carbon nanotubes with different cobalt loading (PdCo1/MWCNT and PdCo2/MWCNT) as anode materials in a microfluidic formic acid fuel cell (μFAFC) using two formic acid concentrations as fuel, and an oxygen-saturated sulfuric acid solution as oxidant. These results are compared to those obtained with pure Pd/MWCNT.

2. Experimental

2.1. PdCo/MWCNT catalyst synthesis

MWCNT-supported PdCo electrocatalysts with a ∼30% metal loading were prepared by the impregnation method. The synthesis and functionalization of MWCNTs were carried out following previously reported procedures [11]. MWCNTs were synthesized by the spray pyrolysis technique [12,13] from toluene (99%, J.T. Baker) and ferrocene (98%, Aldrich) solutions. Argon (Praxair) was injected into the nebulizer as the carrier gas. In this way, a ferrocene/toluene solution was fed into a quartz tube when the temperature of the furnace (Thermoline) reached 900 °C the argon flow was maintained. The MWCNTs were cleaned by refluxing for 12 h at 80 °C in concentrated HNO_3. The solution was filtered and washed with distilled water. Later, the MWCNTs were immersed in a HNO_3/H_2SO_4 (1:4, v/v) solution for 5 h at 60 °C under same refluxing and stirring conditions in order to promote their functionalization. The resulting powder was washed with deionized water until the pH of the rinsing liquid was 7 and then dried overnight at 60 °C. The diameter and length of the MWCNTs obtained ranged between 20 and 80 nm and 300 μm.

MWCNT-supported PdCo catalysts with different Co atomic ratios (PdCo1/MWCNT and PdCo2/MWCNT) were synthesized by impregnation in a high frequency ultrasonic processor (UP400S) at room temperature using $NaBH_4$ as the reducing agent. $(NH_4)_2PdCl_6$ (Stream Chemicals, 99%) and $Co(NO_3)_2{\cdot}6H_2O$ (Alfa Aesar, 98%) were dissolved in deionized water and added to an aqueous dispersion of MWCNTs under continuous ultrasonic stirring for 30 min. $NaBH_4$ (Sigma–Aldrich, 98.5%) was then slowly added to this mixture under vigorous stirring for 30 min. The resulting solution was filtered, washed and dried overnight at 60 °C. Afterwards, the as-prepared catalysts were annealed at 350 °C in a flowing mixture of 10% H_2–90% Ar for 1 h, maintaining a heating rate of 5 °C min^{-1}. For comparison, Pd/MWCNT was prepared using the same synthesis procedure.

2.2. Catalyst characterization

The synthesized catalysts were characterized by X-ray diffraction (XRD) measurements on an X-pert MPD Phillips diffractometer using Cu Kα radiation operating at 40 kV and 35 mA. A JEOL JSM 5800-LV scanning electron microscope was used for SEM image characterization and energy dispersive X-ray (EDX) was used for elemental analysis of the catalysts. High resolution X-ray photoelectron spectroscopy (XPS) measurements were carried out using a ThermoElectron (East Grinstead, UK) instrument with an Alpha 110 electron analyzer under monochromatic Al Kα radiation ($h\nu$ = 1486.7 eV) at 200 W with the pass energy fixed at 15 eV. A low energy flood gun was used to minimize the charging effect. To compensate for surface charging effects, all of the binding energies were referenced to the C1s spectrum of carbon at 284.8 eV.

2.3. Microfluidic fuel cell fabrication, catalyst deposition and cell testing

The μFAFC was made of poly(methyl methacrylate) (PMMA) and machined with the following dimensions: 2 mm width (1 mm for each channel), 1 mm high and 45 mm long, with an electrode area of 0.45 cm^2. Cell construction was carried out using the hot-press method, utilizing PMMA substrates heated at 140 °C and pressed to 24,000 lbs in^{-2}. Anode and cathode current collectors were fabricated using XC72-Vulcan from catalyst inks and were deposited on the walls of graphite electrodes using the spray technique. The inks were prepared by dispersing the catalyst powder in appropriate amount of isopropyl alcohol and Nafion®. Anode catalyst inks were sprayed on one side (wall channel), and the cathodic ink was sprayed on the opposite side [2]. Two different micro fuel cells were constructed in order to compare the effects of Co wt.% in the Pd-based catalyst (PdCo1/MWCNT and PdCo2/MWCNT), and a third cell based on Pd/MWCNT (22 wt.%) was constructed for comparison. Anode catalyst loadings were 1.2 mg cm^{-2}, 1.2 mg cm^{-2} and 1 mg cm^{-2} for PdCo1/MWCNT, PdCo2/MWCNT and Pd/MWCNT, respectively. For the three configurations under study, 0.7 mg cm^{-2} of 30 wt.% Pt/Vulcan (E-TEK) was used as the cathode catalyst. Fig. 1 shows the micro fuel cell structure employed for the catalyst performance evaluation.

Fuel solutions with different formic acid concentrations (0.1 and 0.5 M) in 0.5 M H_2SO_4 and oxygen (4.3 U.A.P. Praxair) dissolved in 0.5 M H_2SO_4 were used as anode and cathode fluids, respectively. An increase in the saturation of oxidant in sulfuric acid media was performed by humidification of the oxygen gas with a saturation tower [2]. The anolyte (fuel in electrolyte) and catholyte (oxidant in electrolyte) streams were fed to the corresponding inlets in laminar flows using a peristaltic pump (Masterflex Cole-Palmer Mod-7553-70). The flow rate and cell dimensions correspond to a Reynolds number of 0.1, assuring laminar flow conditions. In all the fuel cell experiments, the cathode (O_2-purged H_2SO_4) and anode (HCOOH-H_2SO_4) flow rates were kept at 0.43 mL min^{-1} and 0.06 mL min^{-1}, respectively. Voltage and current measurements were performed using an Autolab PGSTAT30 potentiostat/galvanostat. Polarization curves of the individual electrodes (formic acid oxidation and oxygen reduction reactions) were obtained using an external Ag/AgCl reference electrode that was placed close to the outlet stream. The cell performance and individual electrode evaluations were

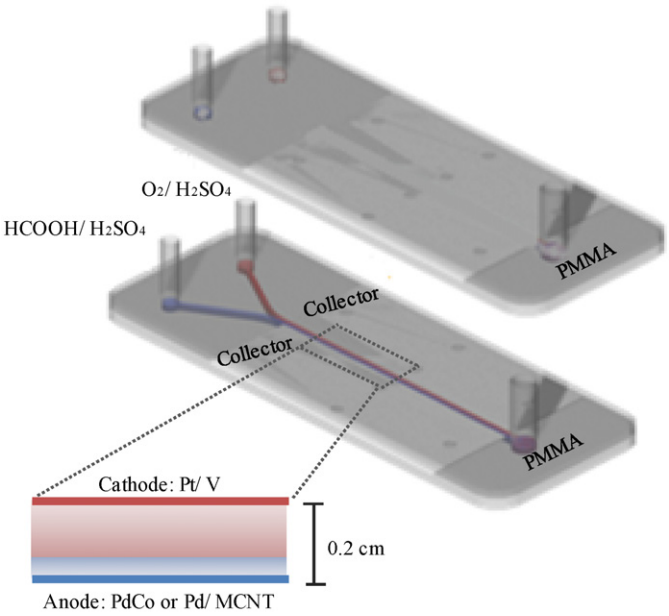

Fig. 1. Schematic diagram of a laminar microfluidic fuel cell.

not adjusted for ohmic drops. All tests were performed at room temperature.

3. Results and discussion

3.1. Physicochemical characterization

The PdCo1/MWCNT, PdCo2/MWCNT and Pd/MWCNT catalyst compositions were determined by EDX analysis as described in the experimental section. The EDX atomic compositions were obtained by taking measurements in several regions of the nanoparticle powders and the results, which are very close to the nominal values, are shown in Table 1.

Fig. 2 on the other hand, compares the XRD patterns of the PdCo1/MWCNT, PdCo2/MWCNT and Pd/MWCNT catalysts. These data indicate the formation of single phase materials with a face-centered cubic structure. The diffraction peaks around 26°, 44° and 54° in all the patterns of the carbon nanotube-supported catalysts are due to the (0 0 2) (1 0 1) and (0 0 4) reflections of the hexagonal structure of carbon. The rest of the peaks observed at about 40°, 47° and 68° are due to the Pd (1 1 1), (2 0 0) and (2 2 0) reflections, respectively. These peaks are typical for the crystalline Pd face-centered cubic (fcc) phase.

It is important to note that the reflections of PdCo1/MWCNT and PdCo2/MWCNT are shifted to higher angles compared to those of Pd/MWCNT (indicated by a dashed line in Fig. 2). This observation confirms the substitution of Co for Pd atoms in the Pd lattice. The alloying degree (x, at.% Co incorporated into the Pd lattice) was estimated from the previously calculated lattice constants of Pd

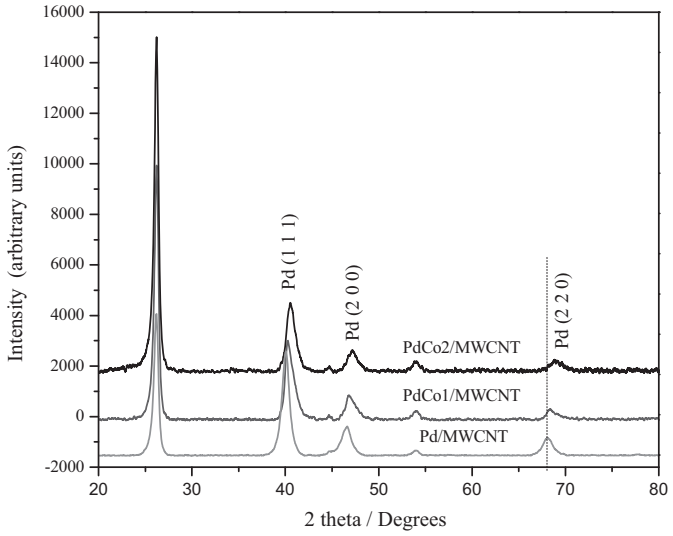

Fig. 2. XRD patterns for Pd-Co/MWCNT alloys and Pd/MWCNT.

(a_{Pd}) and the PdCo alloy (a_{alloy}), and the metallic radii of Co, r_{Co} (1.25 Å) and Pd, r_{Pd} (1.37 Å) using Eq. (1) [15].

$$x\left(1-\frac{w_{Co}}{r_{Pd}}\right)=1-\frac{a_{alloy}}{a_{Pd}} \quad (1)$$

The lattice parameter and crystal size values were obtained from the data corresponding to the (2 2 0) reflections of Pd using the Scherrer relation described in Eq. (2) [16].

$$L=\frac{0.9\lambda}{B_{2\theta}\cos\theta_B} \quad (2)$$

where L is the average particle size, λ is the X-ray wavelength for Cu Kα radiation (1.5406 Å), $B_{2\theta}$ is the peak broadening and θ_B is the angle corresponding to the peak maximum. It is interesting to note that the particle sizes of PdCo1/MWCNT and PdCo2/MWCNT were slightly smaller than that of pure Pd. These values, along with other physicochemical parameters, are reported in Table 1. Inspection of this data suggests that the addition of Co to the Pd lattice can shift the (fcc) Pd crystal lattice parameter (3.889 nm) to slightly smaller values (3.877 and 3.855 nm).

3.2. PdCo anode performance

Voltamperograms of the Pd/MWCNT, PdCo1/MWCNT and PdCo2/MWCNT anodes were obtained in a microfluidic fuel cell using a reference electrode immersed in 0.5 M sulfuric acid and a potential window from −0.2 to 0.9 V, as shown in Fig. 3. Although the three anode electrodes show the characteristic voltamperometric response of Pd in acid media, some differences in the hydrogen adsorption and desorption profiles were observed. In particular, PdCo2/MWCNT exhibited a shifted onset in the potential of oxide reduction relative to that observed for Pd/MWCNT (50 mV).

The fuel cell polarization and power density curves using Pd/MWCNT and two PdCo/MWCNT ratios as anodes in 0.1 and

Table 1
Structural characterization data of the electrocatalysts.

	Pd/MWCNT	PdCo1/MWCNT	PdCo2/MWCNT
Composition Pd:Co/wt.% (EDX)	30	22:7	21:9
Composition Pd:Co/at.% (EDX)	1:0	0.5: 0.5	0.4: 0.6
Cristal size/nm (XRD)[a]	13	8.2	6.5
Lattice parameter XRD (nm)	3.889	3.877	3.855
Surface area S_A ($m^2\ g^{-1}$) (XRD)	38.30	60	77.30
Atomic percent Co in the sample (%)[a]	–	4.23	10.62

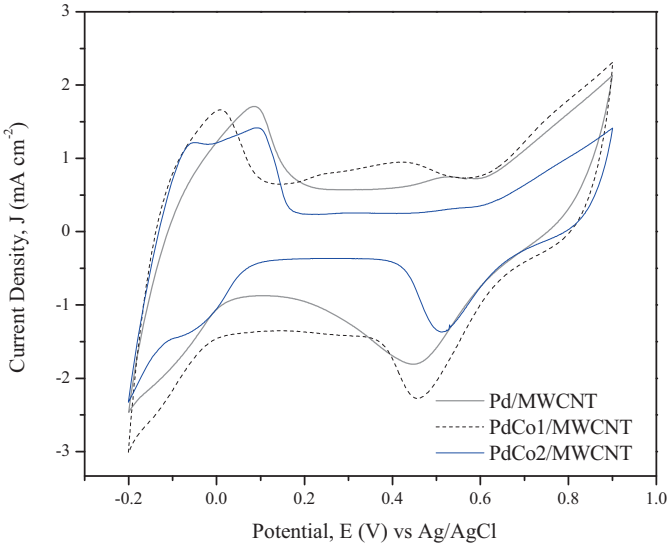

Fig. 3. Cyclic voltammograms of Pd/MWCNT, PdCo1/MWCNT and PdCo2/MWCNT electrodes in 0.5 M H_2SO_4 at a scan rate of 20 mV s^{-1}.

0.5 M formic acid as fuel are shown in Figs. 4a and 5, respectively. In these experiments, the flow rates were kept at 0.06 mL min^{-1} for the anodic and 0.43 mL min^{-1} for the cathodic stream, with a fuel:oxidant rate ratio of 1:7. At these conditions, the best performance for the system was obtained, which was probably because the stream close to the anode reduces fuel crossover due a larger diffusion distance from the cathode. This translates into a substantial impact on the diffusive broadening and depletion layer formation [17].

Although the power density values obtained are below those previously reported (3.3 mW cm^{-2}) [2], it is important to note the decreased cathode catalyst loading (from 1.9 to 0.7 mg cm^{-2} of Pt/V XC-72) for the same amount of catalyst in the anode. The polarization curves recorded for these microfluidic fuel cells on the other hand, have the same characteristic shape of typical fuel cells, with kinetically, ohmic, and mass transport limited regions. At 0.1 M formic acid concentration (Fig. 4a) the open circuit potential (OCP) is 0.84 V when Pd/MWCNT is used as anode and the current density is low as a consequence of mass transport limitations. Consequently, the cell performance is low, achieving only 0.7 mW cm^{-2} (see Table 2). In configurations where PdCo1/MWCNT and PdCo2/MWCNT were used as anodes, higher open circuit potentials were observed (0.89 V for both catalysts). In addition, a noticeable increase in the slope in the mass transport regime of the polarization curves is observed, resulting in higher power density values (see Table 2).

In order to evaluate each single electrode reaction; an external Ag/AgCl reference electrode was incorporated in the microfluidic fuel cell system. The use of an external reference electrode allowed separate analysis and evaluation of individual electrode performance characteristics, to complement the overall cell performance. According to the polarization curves of the individual electrodes (Fig. 4b), the cathode suffers lower polarization losses than the anode, as evidenced by the remarkable difference in the maximum current densities for the anodic reaction (2.7, 7.0 and 5.8 mA cm^{-2} for Pd/MWCNT, PdCo1/MWCNT and PdCo2/MWCNT, respectively).

Fig. 5 shows the polarization curves for the three different electrode materials at a higher concentration of formic acid (0.5 M). From these experiments, it can be seen that while the OCP for the microfluidic fuel cell equipped with Pd/MWCNTs decreased from 0.84 to 0.82 V (Fig. 5a), the other two cells (prepared with PdCo1/MWCNTs and PdCo2/MWCNTs) retained the same OCP. The

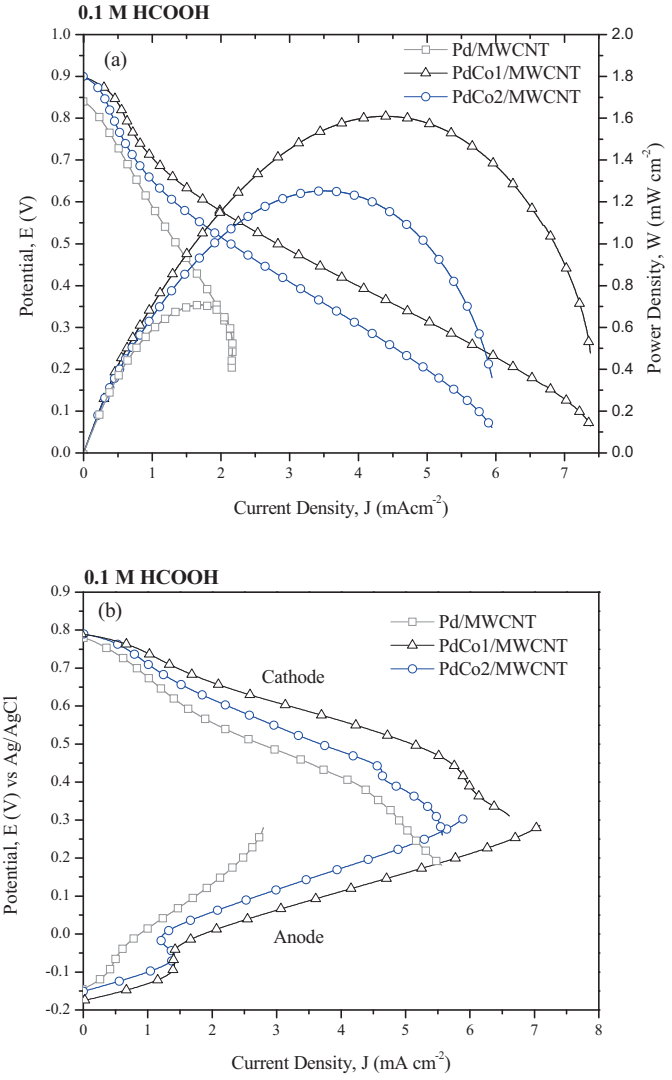

Fig. 4. (a) Polarization and power density curves for Pd/MWCNT, PdCo1/MWCNT and PdCo2/MWCNT in a HCOOH-H_2SO_4/O_2-H_2SO_4 microfluidic fuel cell and (b) anode and cathode polarization curves operating at 0.1 M HCOOH with a flow rate of 0.485 ml min^{-1}.

current density for the Pd/MWCNT cell configuration, on the other hand, increased as a consequence of the higher fuel concentration. Using PdCo1/MWCNT and PdCo2/MWCNT, it was possible to observe an increase in the activation zone, suggesting better catalytic activity for the oxidation reaction (Fig. 5b) and as a consequence, higher power density values (Table 2).

The Pd/MWCNT anode suffers a higher polarization loss, as confirmed by external measurements (Fig. 5b). As a consequence the oxidation potential is change by approximately 0.250 V at the maximum current density, with an increase of formic acid concentration (0.1–0.5 M) corresponding to an increase from 0.26 to 0.51 V. On PdCo electrodes this oxidation potential is unaffected. In addition, the current densities are improved for the three electrodes at a higher fuel concentration, particularly for PdCo2/MWCNT (increasing from 5.8 to 8 mA cm^{-2}). In all three cases, however, the total current density did not increase significantly with a higher fuel concentration (0.5 M), suggesting that the overall performance of the microfluidic fuel cell is limited by the cathodic reaction (Fig. 5a). Even when the current density associated with formic acid oxidation is increased for PdCo anode electrodes at 0.5 M HCOOH (Fig. 5a) the microfluidic fuel cell performance is mainly affected by the low oxygen concentration in acid media. These observations suggest

Table 2
Peak power density and current density of the μFAFC for three anodes configurations.

HCOOH (M)	Pd/MWCNT			PdCo1/MWCNT			PdCo2/MWCNT		
	E_{max} (V)	J_{max} (mA cm^{-2})	W_{max} (mW cm^{-2})	E_{max} (V)	J_{max} (mA cm^{-2})	W_{max} (mW cm^{-2})	E_{max} (V)	J_{max} (mA cm^{-2})	W_{max} (mW cm^{-2})
0.1	0.84	2.1	0.7	0.89	7.3	1.6	0.89	5.95	1.26
0.5	0.82	2.9	0.85	0.9	5.9	1.75	0.89	4.6	1.5

that the overall performance of the microfluidic fuel cell is limited by the cathodic reaction (Fig. 5a).

To understand the effects of Co alloying, XPS measurements were performed to determine the chemical states of the catalyst surfaces. High resolution Pd 3d XPS spectra for Pd/MWCNT, PdCo1/MWCNT and PdCo2/MWCNT electrocatalysts are shown in Fig. 6a, b and c, respectively. The spectra were fitted and evaluated simultaneously in the Analyzer software [14] using a mixed Gaussian–Lorentzian function. The binding energy (BE) separation between Pd $3d_{5/2}$ and Pd $3d_{3/2}$ lines was fixed to 5.30 eV according to empirical determinations. The reported BE is associated with the Pd $3d_{5/2}$ line. De-convolution of the Pd 3d signal was achieved using three doublets, which indicates the existence of at least three forms of Pd. The main constituent was Pd metallic (Pd^{+}) at a BE of 335.1 eV for Pd/MWCNT and 335.5 eV for both PdCo1/MWCNT and PdCo2/MWCNT samples [18]. The doublet at 335.7 eV for Pd/MWCNT and at 336.3 eV for PdCo1/MWCNT and PdCo2/MWCNT can be attributed to PdO_{ads} species, and the doublet at higher BE values, at 337.4 eV, 337.6 and 337.9 for Pd/MWCNT, PdCo1/MWCNT and PdCo2/MWCNT samples respectively, corresponds to PdO or Pd-$(OH)_2$ [18]. The shape of this last doublet suggests partial reduction of the palladium for PdCo/MWCNT alloys, although a small fraction remained oxidized. According to previous reports, avoiding the formation of Pd oxides on the surface contributes to improvement of the catalytic activity of Pd-based alloys [19]. For both PdCo/MWCNT alloys the position of the Pd^{+} peak is shifted by 0.4 eV toward higher BEs with respect to the Pd/MWCNT sample. This shift could be attributed to the chemical interaction between Pd and Co elements [18]. Similar behavior was observed in previous work by Lee et al. [19] for a $Pd_{60}Co_{40}$ electrocatalyst, where they reported a shift of 0.4 eV to higher BEs for the Pd alloy compared to pure Pd. Previous reports also describe the relationship of the degree of hybridization to shifts of the core-level BEs [20,21]. For PdCo/MWCNT catalysts, the BE shifts originate from the *d*-band hybridization between Pd and Co upon alloying because *d*-orbitals form stronger bonds between metal atoms, reducing the potential to form strong bonds with adsorbed reactants [4]. Furthermore,

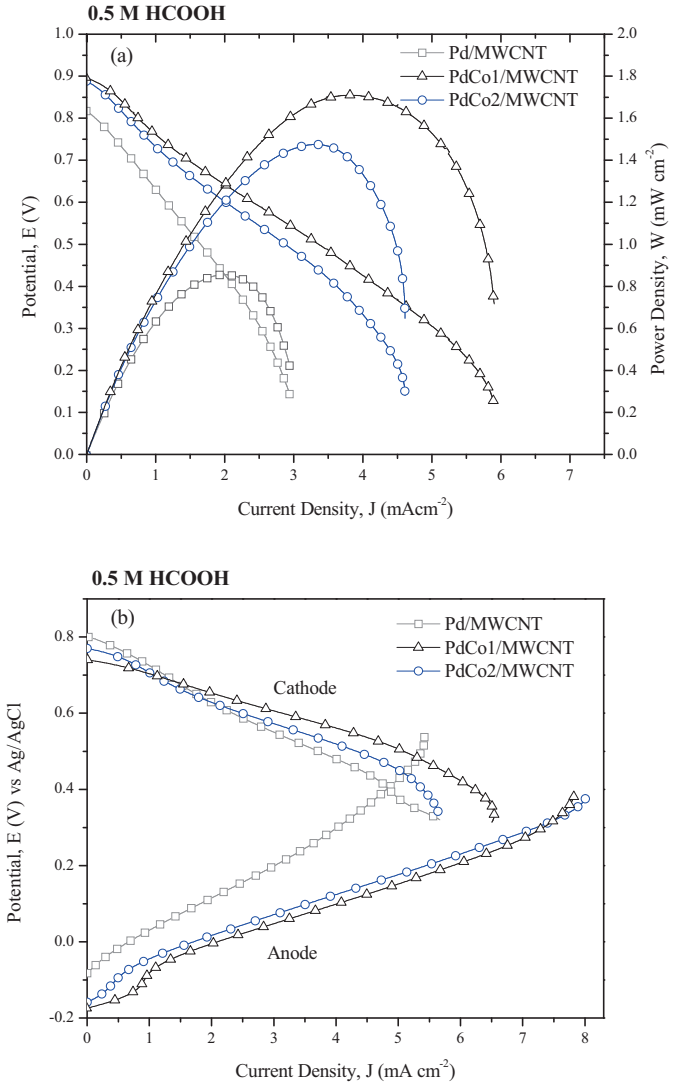

Fig. 5. (a) Polarization and power density curves for Pd/MWCNT, PdCo1/MWCNT and PdCo2/MWCNT in a HCOOH-H_2SO_4/O_2-H_2SO_4 microfluidic fuel cell and (b) anode and cathode polarization curves operating at 0.5 M HCOOH with a flow rate of 0.485 ml min^{-1}.

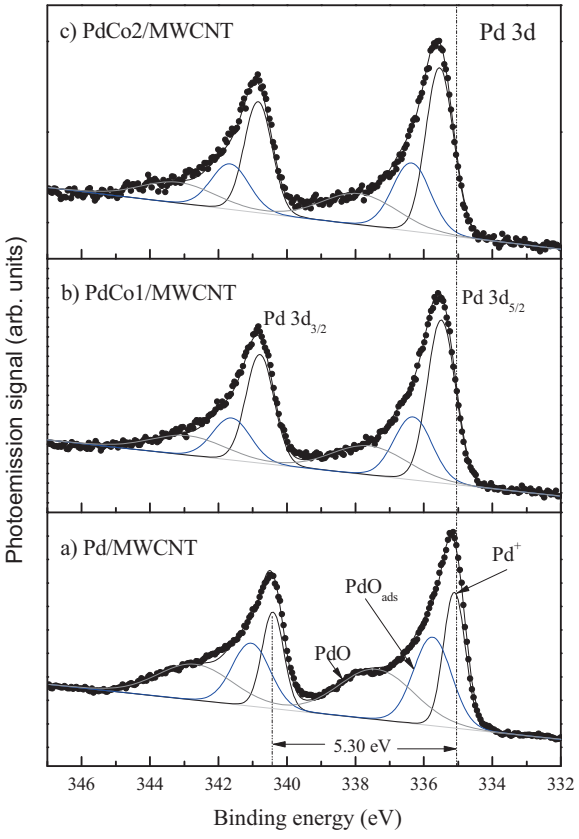

Fig. 6. XPS spectra corresponding to the Pd 3d binding energy region for (a) Pd/MWCNT, (b) PdCo1/MWCNT and (c) PdCo2/MWCNT electrocatalysts.

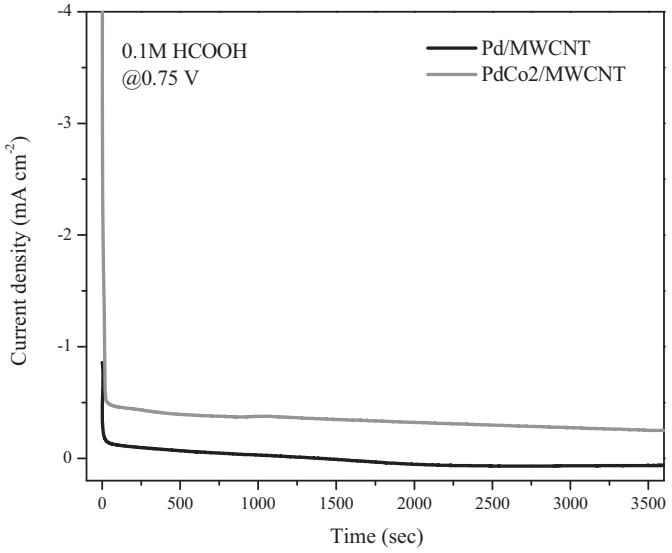

Fig. 7. Current density as a function of time for Pd/MWCNT and PdCo2/MWCNT anode configurations at 0.75 V for a microfluidic fuel cell using 0.1 M HCOOH.

the BE shift indicates that the density of states (DOS) at the Fermi level decreases upon filling the Pd *d*-band, as electron density is transferred from Co to Pd atoms [22]. As the Pd *d*-band is filled by electrons donated by Co, the corresponding chemisorption of O and OH species on the electrode surface gets weaker [19]. Thus, the DOS at the Fermi level affects the chemisorption of O and OH species on the surface and the electrocatalytic activity. Particularly for the formic acid reaction, the shifts observed in Pd 3d binding energy values for both PdCo/MWCNT alloys suggest that the formic acid oxidation reaction occurs with low or negligible adsorption of the intermediate $COOH_{ads}$ [19].

Even when formic acid electro-oxidation on the Pd catalyst occurs preferentially via the direct pathway [1], intermediates produced during this process could be absorbed on Pd or PdCo surfaces and poison their catalytic activity and stability. To demonstrate that, on the PdCo2/MWCNT surface, the intermediaries of reaction produced during the oxidation are adsorbed less than on Pd/MWCNTs, and to investigate how these intermediates affect catalytic activity and stability, we performed chronoamperometric studies with PdCo catalysts in a microfluidic fuel cell. The chronoamperometric measurements were performed at 0.75 V in a microfluidic fuel cell with 0.1 M formic acid and PdCo2/MWCNT and Pd/MWCNT anode configurations for 3600 s (Fig. 7). The resulting curves indicate that the PdCo2/MWCNT electrode has a superior current density, 0.27 mA cm^{-2}, after 3600 s, while Pd/MWCNT exhibited only 0.055 mA cm^{-2}. The decreased catalytic activity in Pd/MWCNT is probably due to the adsorption of intermediates and/or deactivation. PdCo1/MWCNT, on the other hand, exhibited the same performance as PdCo2/MWCNT (data not shown).

According to the preceding results, the improvement of both PdCo/MWCNT catalysts in the microfluidic fuel cell compared to Pd/MWCNT may be attributed to several factors. The first is related to changes in lattice parameter due to the incorporation of Co into the Pd lattice as well as to decreased particle size and increased surface area. Based on XPS results, the changes in binding energy of PdCo1/MWCNT and PdCo2/MWCNT due to the interaction of Pd with Co could result in a decrease in the adsorption energy of the intermediate (formate), favoring the desired oxidation reaction. Furthermore, the improvement in catalytic stability can be related to the atomic percentage of Co in the sample (alloying degree). Based on Fig. 5b (anode electrode curve), PdCo2/MWCNT has the same catalytic activity in comparison with PdCo1/MWCNT, using a lower Pd loading with a larger alloying degree.

4. Conclusions

PdCo1/MWCNT and PdCo2/MWCNT alloys were studied as novel anodes in a microfluidic formic acid fuel cell. We have demonstrated the successful incorporation of Co in a Pd catalyst, which is reflected by a shift in BE with respect to pure Pd and by the lattice parameters obtained. Improved performance was obtained for the cell equipped with PdCo1/MWCNT (1.75 mW cm^{-2}) when compared to Pd/MWCNT (0.85 mW cm^{-2}) using 0.5 M HCOOH. Through external electrode measurements it was possible to determine that PdCo2/MWCNT has a better catalytic activity (8 mA cm^{-2}) and inhibited deactivation with a higher concentration of formic acid. Making a correlation between the electrocatalytic activity and structural changes, the most active catalyst is composed of the smallest PdCo nanoparticles (6.5 nm), which implies that there is a direct relationship between catalytic stability and the percentage of Co in the sample (alloying degree). In more general terms, both PdCo/MWCNT alloys exhibit superior catalytic activity and stability in comparison to pure Pd/MWCNT.

Acknowledgments

The authors acknowledge financial support from the Mexican Council for Science and Technology (CONACyT, Fomix-Chihuahua 127461). We also thank to M. Roman, E. Torres and K. Campos for technical support in XRD and SEM measurements.

References

[1] E.R. Choban, J.S. Spendelow, L. Gancs, A. Wieckowski, P.J.A. Kenis, Electrochim. Acta 50 (2005) 5390–5398.
[2] D. Morales-Acosta, H. Rodríguez, G. Luis, A. Godinez, L.G. Arriaga, J. Power Sources 195 (2010) 1862–1865.
[3] A. Capon, R. Parsons, J. Electroanal. Chem. 45 (1973) 205–231.
[4] W.P. Zhou, A. Lewera, R. Larsen, R.I. Masel, P.D. Bagus, A. Wieckowski, J. Phys. Chem. B 110 (2006) 13393–13398.
[5] L.A. Kibler, A.M. El-Aziz, D.M. Kolb, J. Mol. Catal. A: Chem. 199 (2003) 57.
[6] T. Shobha, C.L. Aravinda, P. Bera, L.G. Devi, S.M. Mayanna, Mater. Chem. Phys. 80 (2003) 656.
[7] R.S. Jayashree, J.S. Spendelow, J. Yeom, C. Rastogi, M.A. Shannon, P.J.A. Kenis, Electrochim. Acta 50 (2005) 4674.
[8] X. Wang, Y. Tang, Y. Gao, T. Lu, J. Power Sources 175 (2008) 784.
[9] X. Yu, P.G. Pickup, J. Power Sources 192 (2009) 279–284.
[10] Z. Liu, X. Zhang, Electrochem. Commun. 11 (2009) 1667–1670.
[11] D. Morales-Acosta, J. Ledesma-Garcia, L.A. Godinez, H.G. Rodríguez, L. Álvarez-Contreras, L.G. Arriaga, J. Power Sources 195 (2010) 461–465.
[12] D.H. Galvan, A. Aguilar-Elguézabal, G. Alonso, Opt. Mater. 29 (2006) 140–143.
[13] G. Alonso-Nuñez, A.M. Valenzuela-Muñiz, F. Paraguay-Delgado, A. Aguilar, Y. Verde, Opt. Mater. 29 (2006) 134–139.
[14] A. Herrera-Gómez, et al., Phys. Rev. B 61 (2000) 12988–12991.
[15] Y. Suo, L. Zhuang, J. Lu, Angew. Chem. Int. Ed. 46 (2007) 2862–2864.
[16] B.E. Warren, X-Ray Diffraction, Addison-Wesley, Reading, MA, 1996.
[17] R.S. Jayashree, S.K. Yoon, F.R. Brushett, P.O. Lopez-Montesinos, D. Natarajan, L.J. Markoski, P.J.A. Kenis, J. Power Sources 195 (2010) 3569–3578.
[18] K.S. Kim, A.F. Gossmann, N. Winograd, Anal. Chem. 46 (1974) 197–204.
[19] K. Lee, O. Savadogo, A. Ishihara, S. Mitsushima, N. Kamiya, K. Ota, J. Electrochem. Soc. 153 (2006) A20–A24.
[20] B. Richter, H. Kuhlenbeck, H.J. Freund, P.S. Bagus, Phys. Rev. Lett. 93 (2004) 026805.
[21] P.S. Bagus, A. Wieckowski, H.J. Freund, Chem. Phys. Lett. 420 (2006) 42–46.
[22] G.N. Derry, P.N. Ross, Solid State Commun. *52* (1984) 151.